Microporous Decatungstates: Synthesis and Photochemical Behavior

Yihang Guo, Changwen Hu,* Xinlong Wang, Yonghui Wang, and Enbo Wang

Institute of Polyoxometalate Chemistry, Faculty of Chemistry, Northeast Normal University, Changchun 130024, People's Republic of China

Yongcun Zou, Hong Ding, and Shouhua Feng

Key Laboratory of Inorganic Synthesis and Preparative Chemistry, Jilin University, Changchun 130023, People's Republic of China

Received March 9, 2001. Revised Manuscript Received July 20, 2001

Photoreactive decatungstates $Na_4W_{10}O_{32}$ and $(nBu_4N)_4W_{10}O_{32}$ were heterogenized inside the silica network via a sol−gel technique, resulting in the $Na_4W_{10}O_{32}/SiO_2$ (Na**1**) and $(nBu_4N)_4W_{10}O_{32}/SiO_2$ (Q**1**) composites. The physicochemical properties of as-synthesized composites were measured by UV diffuse reflectance spectrum, Fourier transform infrared, thermogravimetric analysis and differential thermal analysis, inductively coupled plasma-atomic emission spectroscopy, and scanning electron micrograph, suggesting that the structural integrity of the decatungstates has been preserved after incorporation into the silica network. The microporous structures of the Na**1** and Q**1** were confirmed by the nitrogen adsorption measurements. The photocatalytic behaviors of the composites were studied via degradation and mineralization of organophosphorus pesticide, trichorofon (TCF), under near-UV irradiation and in media where they are insoluble. The photocatalytic behaviors of the Na**1** and Q**1** were also compared with two silica-supported decatungstates, $Na_4W_{10}O_{32}-SiO_2$ (Na**2**) and $(nBu_4N)_4W_{10}O_{32}-SiO_2$ (Q**2**). It indicated that the Na**1** had the highest photocatalytic efficiency among four insoluble decatungstates, and the leakage of the catalyst from the support was hardly observed for Na**1**. Studies on the reaction mechanism indicate that $OH^{\bullet}$ radical attack may be responsible for the degradation and final mineralization of TCF.

Introduction

The intrinsic thermal redox and photoredox activities of polyoxometalates (POMs) are well-known.[1−10] Up until now, much work has been done on studying POMs as heterogeneous thermal catalysts and applying them for industrial purposes.[11−13] However, most of studies on photooxidative behavior of POMs have been made with homogeneous solutions.[14−19] The major drawback to the practical applications of these systems is the high water solubility of POM, which impedes ready recovery and reuse of the photocatalysts (and therefore, its cost-effectiveness). Furthermore, active sites on the surface are small because of the low specific surface areas of solid POMs (ca. 5 $m^2\ g^{-1}$). Recently, progress has been made in preparation of the desolubilized POMs for the purposes of photooxidation of aqueous pollutants via (1) support or inclusion of Keggin-type POMs on a silica matrix,[20−22] (2) preparation of POM-containing layered double hydroxides,[23] and (3) precipitation with large countercations such as Cs^+.[24−26] Most of insoluble POMs

* To whom correspondence should be addressed. Telephone or fax: +86-431-5640694. E-mail: huchw@nenu.edu.cn.

(1) Okuhara, T.; Mizuno, N.; Misono, M. *Adv. Catal.* **1996**, *41*, 113.
(2) Yamase, T.; Takabayashi, N.; Kaji, M. *J. Chem. Soc., Dalton Trans.* **1984**, 793.
(3) Chemseddine, A.; Sanchez, C.; Livage, J.; Launay, J. P.; Fournine, M. *Inorg. Chem.* **1984**, *23*, 2609.
(4) Renneke, R. F.; Hill, C. L. *J. Am. Chem. Soc.* **1988**, *110*, 5461.
(5) Papaconstantinou, E. *Chem. Soc. Rev.* **1989**, *18*, 1.
(6) Stattari, D.; Hill, C. L. *J. Chem. Soc., Chem. Commun.* **1990**, 634.
(7) Stattari, D.; Hill, C. L. *J. Am. Chem. Soc.* **1993**, *115*, 4649.
(8) Tanielian, C. *Coord. Chem. Rev.* **1998**, *178−180*, 1165.
(9) Duncan, D. C.; Netzel, T. L.; Hill, C. L. *Inorg. Chem.* **1995**, 4640.
(10) Okuhara, T.; Watanabe, H.; Nishimura, T.; Lnumaru, K.; Misono, M. *Chem. Mater.* **2000**, *12*, 2230.
(11) Okuhara, T.; Nishimura, T.; Watanabe, H.; Misono, M. *Stud. Surf. Sci. Catal.* **1994**, *90*, 419.
(12) Lee, K. Y.; Arai T.; Nakata, S.; Asaoka, S.; Okuhara T.; Misono, M. *J. Am. Chem. Soc.* **1992**, *114*, 2863.
(13) Izumi, Y.; Ono, M.; Kitagawa, M.; Yoshida M.; Urabe, K. *Microporous Mater.* **1995**, *5*, 255.
(14) Einaga, H.; Misono M. *Bull. Chem. Soc. Jpn.* **1997**, *70*, 1551.
(15) Hou, Y.; Hill C. L. *New J. Chem.* **1992**, *16*, 909.
(16) Yamase, T.; Usami, T. *J. Chem. Soc., Dalton Trans.* **1998**, 183.
(17) Mylonas, A.; Papaconstanitinou, E. *J. Photochem. Photobiol. A* **1996**, *94*, 77.
(18) Ozer, R. R.; Ferry, J. L. *J. Phys. Chem. B* **2000**, *104*, 9444.
(19) Hu, C.; Yue, B.; Yamase, T. *Appl. Catal. A* **2000**, *194*, 99.
(20) Molinari, A.; Amadelli, R.; Andreotti, L.; Maldotti, A. *J. Chem. Soc., Dalton Trans.* **1999**, 1203.
(21) Molinari, A.; Amadelli, R.; Carassiti, V.; Maldotti, A. *Eur. J. Inorg. Chem.* **2000**, 91.
(22) Guo, Y.; Wang, Y.; Hu, C.; Wang, E. *Chem. Mater.* **2000**, *12*, 3501.
(23) Guo, Y.; Li, D.; Hu, C.; Wang, Y.; Wang, E. *Appl. Catal. B* **2001**, *3−4*, 337.
(24) Friesen, D. A.; Morello, L.; Headley, J. V.; Langford, C. H. *J. Photochem. Photobiol. A* **2000**, *133*, 213.
(25) Friesen, D. A.; Headley, J. V.; J. V.; Langford, C. H. *Environ. Sci. Technol.* **1999**, *33*, 3193.
(26) Friesen, D. A.; Gibson D. B.; Langford, C. H. *J. Chem. Soc., Chem. Commun.* **1998**, 543.

10.1021/cm010211i CCC: $20.00
Published on Web 10/13/2001

have micro- or mesoporous structures, so that they have much higher surface areas compared with their parent POMs. Therefore, the photocatalytic activity of these porous solids was expected to be increased significantly because of better spreading of the active sites on the supports.[27] At the same time, they are easily handled for recycling uses. However, in the cases of the colloid catalysts such as semiconductor TiO_2 ultrafine particles and $Cs_xH_{3-x}PW_{12}O_{40}$, it is difficult to separate them from the treated aqueous solution due to formation of milky dispersion.

Here, we prepared insoluble and easily separated microporous decatungstates $Na_4W_{10}O_{32}/SiO_2$ (Na**1**) and $(nBu_4N)_4W_{10}O_{32}/SiO_2$ (Q**1**) (Q = nBu_4^+) by a sol−gel technique via hydrolysis of tetraethyl orthosilicate (abbreviated TEOS) in the presence of inorganic precursors, $Na_4W_{10}O_{32}$ and $(nBu_4N)_4W_{10}O_{32}$. The reasons for choosing decatungstates as the photocatalytic materials are as follows. First, their UV maximum absorption band appears at 320−324 nm. The band overlaps the solar spectrum and is similar to that of TiO_2.[29] Therefore, they are among the most photochemically active polyoxometalates and are better candidates of the photocatalytic materials than Keggin-type POMs (UV absorption band appears at 260−265 nm).[10] Second, photoreduction produces one- or two-electron blue species that are reoxidized rapidly by oxygen.[2,5] The physicochemical properties of as-synthesized composites were measured by UV diffuse reflectance spectrum (UV/DRS), Fourier transform infrared (FT-IR), thermogravimetric analysis (TGA) and differential thermal analysis (DTA), inductively coupled plasma-atomic emission spectroscopy (ICP-AES), scanning electron micrograph (SEM), and nitrogen adsorption. The results show that the microporous decatungstates have very high BET surface areas and their particle sizes are in the range of 20−40 nm.

Photocatalytic technique has been extensively used to degrade and mineralize organic pollutants in wastewater and has exhibited potential applications for industrial purposes.[30−40] Particularly, pesticides have been considered to be one of the major pollutants to which it is promising to apply photocatalysis.[41,42] Many pesticides cannot be degraded by conventional biological methods, whereas complete mineralization can be achieved by photocatalysis.[43,44] For example, total mineralization of an aqueous organocholorine pesticide, hexachlorocyclohexane, had been achieved with microporous Keggin-type POMs.[22] Here, we have tested the photocatalytic activity of as-synthesized composites by degradation and mineralization of organophosphorus pesticide, TCF (1-hydroxyl-2,2,2-trichloroethylphosphonate-*o*,*o*-dimethyl ester) under near-UV irradiation and in media where they are insoluble. In addition, their photochemical behavior was compared with the silica-supported decatungstates $Na_4W_{10}O_{32}-SiO_2$ (Na**2**) and $(nBu_4N)_4W_{10}O_{32}-SiO_2$ (Q**2**). The highest photocatalytic activity was achieved for Na**1,** and there is no catalyst leakage for Na**1** during the photocatalytic process. Pathway and mechanism of photocatalytic degradation of TCF over Na**1** were inferred according to IC and LC-MS analyses.

Experimental Section

Materials. 1-Butanol, TEOS, $HClO_4$, acetonitrile, dimethylformamide, $Na_2WO_4{\cdot}2H_2O$ and tetrabutylammonium bromide (QBr) were of analytical grade. Doubly distilled water was used in all experiments. TCF was certified reference materials purchased from the State Bureau of Technical Supervision, People's Republic of China. The stock solution of TCF (1000 mg/L) was prepared by dissolving it in CH_3CN in order to avoid its decomposing in aqueous solution. TCF solutions used for the tests were diluted with water to suitable concentrations.

Preparation of the $Na_4W_{10}O_{32}/SiO_2$ and $Q_4W_{10}O_{32}/SiO_2$ Composites. $Na_4W_{10}O_{32}$ and $Q_4W_{10}O_{32}$ were prepared according to published procedures and characterized by UV−vis and FT-IR spectroscopy.[3,10] A 1 g amount of $Na_4W_{10}O_{32}$ or $Q_4W_{10}O_{32}$ was dissolved in a suitable solvent (5 mL of H_2O or a small amount of CH_3CN and 5 mL of H_2O, respectively), and then the acidity of the solution was adjusted to pH 2.0 ± 0.2 with 1.5 mol/L of $HClO_4$. Then, the obtained $W_{10}O_{32}^{4-}$ solution was added dropwise to the mixture of 5 mL of TEOS and 4.5 mL of 1-butanol. The mixture was stirred 1 h at room temperature, then 3 h at 45 °C, and finally 1 h at 80 °C until the hydrogel was formed. Acidity of the mixture was maintained at pH 2.0 ± 0.2 by adding $HClO_4$ during solation. The hydrogel was dehydrated slowly at 45 °C for 12 h and then dried in a vacuum at 80 °C for 6 h. The dried gel was washed with hot water three times and then dried at 80 °C for 6 h, which resulted in the silica particulate gel. Before catalytic application, the particulate gel was calcined in a vacuum at 150 °C for 2 h to fasten the silica network.

Preparation of the $Na_4W_{10}O_{32}/SiO_2$ and $(nBu_4N)_4W_{10}O_{32}/SiO_2$ Composites. Na**2** and Q**2** were prepared by the modified reference methods.[20,21] A 1 g amount of $Na_4W_{10}O_{32}$ or $Q_4W_{10}O_{32}$ was dissolved in a suitable solvent (H_2O or CH_3CN, respectively), and the acidity of the solution was adjusted to pH 2.0 ± 0.2. Subsequently, 10 g of colloidal silica was added. After stirring the slurry for 12 h, the solvent was evaporated and the product was obtained.

Photoreactor and Photocatalytic Procedure. The photoreactor was designed with an internal light source surrounded by a quartz jacket. The temperature of the liquid/solid suspension was maintained at 20 ± 2 °C by circulation of water through an external cooling coil. The optical path length was about 2 cm. The light source was a 125 W high-

(27) Cavani, F. *Catal. Today* **1998**, 73.
(28) Okuhara, T.; Nishimura, T.; Misono, M. *11th International Congress on Catalysis—40th Anniversary*; Elsevier Science B.V.: Amsterdam, 1996; p 581.
(29) Texier, I.; Giannotti, C.; Malato, S.; Richter, C.; Delaire, J. *Catal. Today* **1999**, *54*, 297.
(30) Herrmann, J. M.; Guillard, C.; Arguello, M.; Aguera, A.; Tejedor, A.; Piedra, L.; Fernandez-Alba, A. *Catal. Today* **1999**, *54*, 353.
(31) Assabane, A.; Ichou, Y. A.; Tahiri, H.; Guillard, C.; Herrmann, J. M. *Appl. Catal. B* **2000**, *24*, 71.
(32) Zaleska, A.; Hupka, J.; Wiergowski, M.; Biziuk, M. *J. Photochem. Photobiol. A* **2000**, *135*, 213.
(33) Wang, K.; Hsieh, Y.; Chou, M.; Chang, C. *Appl. Catal. B* **1999**, *21*, 1.
(34) Doong, R.; Chang, W. *J. Photochem. Photobiol. A* **1997**, *107*, 239.
(35) Tanaka, K.; Robledo, S. M.; Hisanaga, T.; Ali, R.; Ramli, Z.; Bakar, W. A. *J. Mol. Catal. A* **1999**, *144*, 425.
(36) D'ollveira, J.-C.; Al-Sayyed, G.; Pichat, P. *Environ. Sci. Technol.* **1990**, *24*, 990.
(37) Herrmann, J.-M. *Catal. Today* **1999**, *53*, 115.
(38) Malato, S.; Blanco, J.; Richter C.; Maldonado, M. I. *Appl. Catal. B* **2000**, *25*, 31.
(39) O'Shea K. E.; Beightol, S.; Garcia, I.; Aguilar, M.; Kalen, D. V.; Cooper, W. J. *J. Photochem. Photobiol. A* **1997**, *107*, 221.
(40) Hoffmann, M. R.; Martin, S. T.; Choi, W. Y.; Bahnemann, D. W. *Chem. Rev.* **1995**, *95*, 69.
(41) Torimoto, T.; Ito, S.; Kuwabata, S.; Yoneyama, H. *Environ. Sci. Technol.* **1996**, *30*, 1275.
(42) Ollis, D. F.; Pelizzetti, E.; Serpone, N.; *Environ. Sci. Technol.* **1991**, *25*, 1522.
(43) Legrini, O.; Oliveros, E.; Braun, A. M. *Chem. Rev.* **1993**, *93*, 671.
(44) Pramaur, E.; Vincenti, M.; Augugllaro, V.; Palmisano, L. *Environ. Sci. Technol.* **1993**, *27*, 1709.

pressure mercury lamp (abbreviated HPML; output mainly at 313.2 nm).

A general photocatalytic procedure was carried out as follows. A 0.2 g amount of catalyst was suspended in a fresh aqueous solution of TCF. The suspension (70 mL) of the catalyst and aqueous TCF was ultrasonicated for 10 min and stirred in the dark for 30 min to obtain a good dispersion. The lamp was inserted into the suspension after its intensity became stable. The suspension was vigorously stirred during the process. All degradation experiments were carried at room temperature, with the photoreactor open to air and at natural pH (ca. 6).

Physical Measurement. The loads of $Na_4W_{10}O_{32}$ or $Q_4W_{10}O_{32}$ in Na**1**, Q**1**, Na**2**, or Q**2** were estimated by a Leeman Plasma Spec (I) ICP-AES. UV, UV/DR, and IR spectra were recorded on a Shimadzu UV-2201 UV−vis spectrophotometer and a Nicolet Magna 560 IR spectrophotometer, respectively. TGA and DTA were performed on a P-E TG 7 thermal analysis system. Nitrogen adsorption measurements were performed at −196 °C by using an ASAP 2010M surface analyzer, and the pretreatment temperature was 180 °C. Scanning electron micrograph images were obtained on a Hitachi S-570 scanning electron microscope.

The photocatalytic activity of as-synthesized materials was tested via monitoring of the changes of the concentration of the product Cl^- ion in the reaction system. TCF is relatively unstable in aqueous solution, while the product $H_2PO_4^-$ ion strongly adsorbed on the surface of the catalyst under acidic condition. Therefore, neither TCF nor $H_2PO_4^-$ ions can be determined accurately. Evolution of inorganic ions (Cl^- and $H_2PO_4^-$) and organic acids (formic acid and acetic acid) was followed by a DX-300 ion chromatograph (IC) equipped with a conductivity detector and an AS4A-SC anion column. Evolution of CO_2 was followed by a reference method.[22] Other highly polar and less volatile intermediate products in aqueous solution were identified by LCQ electrospray mass spectrometer (ES-MS).

Results and Discussion

Preparation and Characterization. Na**1** and Q**1** composites were prepared via a sol−gel technique. The process included hydrolysis of TEOS in the presence of $W_{10}O_{32}^{4-}$ ion at pH 2.0 ± 0.2. When pH is higher than 3.0, $W_{10}O_{32}^{4-}$ ion begins to decompose.[45] $W_{10}O_{32}^{4-}$ ion was entrapped into the silica network during TEOS hydrolysis and then formed microporous decatungstates by subsequent dehydration. The total reaction is presented in

$$M_4W_{10}O_{32} + (C_2H_5)_4OSi + H_2O \xrightarrow{H^+} M_4W_{10}O_{32}/SiO_2 + C_2H_5OH \quad (1)$$

where $M = Na^+$ or nBu_4N^+.

Formation of microporous decatungstates is due to the chemical interaction between the $M_4W_{10}O_{32}$ molecule and the silica network. That is, chemically active silanol group (≡Si−OH) was protonated in an acidic medium to form the ≡Si−OH_2^+ group; the process is described in

$$\equiv Si-OH + H^+ \rightarrow \equiv Si-OH_2^+ \quad (2)$$

The ≡Si−OH_2^+ group should act as a counterion for the $W_{10}O_{32}^{4-}$ ion and yielded (≡Si−OH_2^+)($M_3W_{10}O_{32}^-$) by acid−base reaction. This interaction also exists in microporous $H_3PW_{12}O_{40}/SiO_2$ and $H_4SiW_{12}O_{40}/SiO_2$.[22] In addition, $W_{10}O_{32}^{4-}$ ion is extremely photoreactive, and it can be reduced by some organics such as 1-BuOH to photoinsensitive blue complex ($W_{10}O_{32}^{5-}$ or $W_{10}O_{32}^{6-}$) even under irradiation with natural sunlight. Selecting $HClO_4$ but not HCl to adjust the acidity of the mixture can avoid forming the blue species.

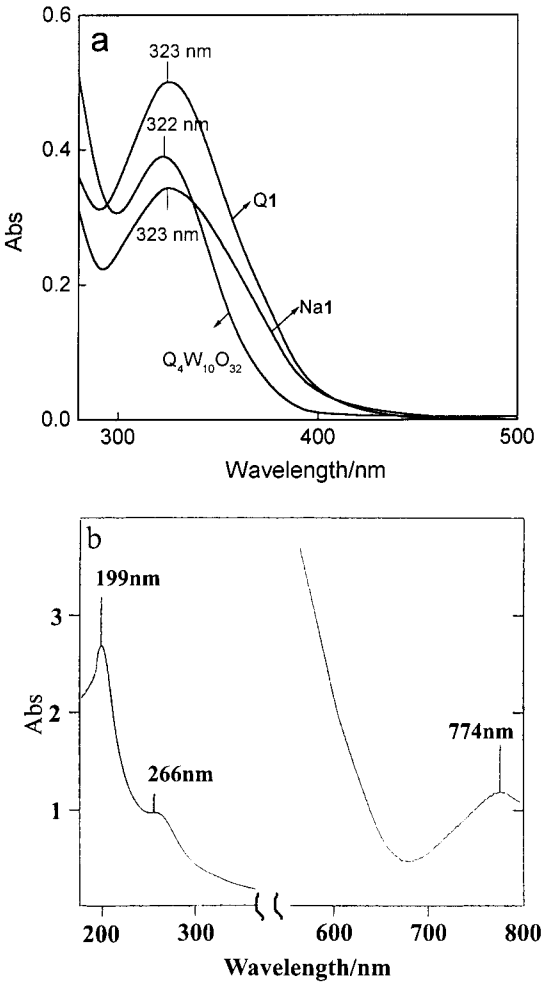

Figure 1. (a) UV or UV/DRS spectra of $Q_4W_{10}O_{32}$, Na**1**, and Q**1**; (b) UV−vis spectrum of the treated solution separated by centrifugation. Irradiation time was 4 h; Q**1** was used.

The load of $Na_4W_{10}O_{32}$ or $Q_4W_{10}O_{32}$ in Na**1**, Q**1**, Na**2**, or Q**2** was ca. 8% estimated by ICP-AES. Na**1** and Q**1** have the UV absorption maximum at 323 nm (Figure 1a), similar to that of the starting decatungstates (λ_{max} = 322 nm), indicating that the structure integrity of the decatungstates has been preserved after incorporation into the silica network. Absorption at ca. 320 nm is characteristic of the $W_{10}O_{32}^{4-}$ cluster, attributed to oxygen-to-tungsten charge transfer (O→W CT) at nearly linear W−O−W bonds (tungsten-bridging oxygen bonds). The IR fingerprint in the region from ca. 1000 to 450 cm^{-1} for Na**1**, Q**1**, Na**2**, and Q**2** is in agreement with that of the starting $W_{10}O_{32}^{4-}$ cluster basically (Table 1), also indicating that the structural integrity of $W_{10}O_{32}^{4-}$ cluster has been preserved. As for the silica framework, its characteristic IR vibration bands mainly appear at 1080 (Si−O−Si), 950 (Si−OH), and 800 cm^{-1} (Si−O−Si). The intense and broad Si−O−Si vibrations covered the vibrations of W═O bond in Na**1**, Q**1**, Na**2**, and Q**2**, and therefore, these vibration bands were not detected. As for the Na**1** and Q**1**, shifting and broadening of the

(45) Hastings, J. J.; Howarth, O. W. *J. Chem. Soc., Dalton Trans.* **1992**, 209.

Table 1. IR Data for Decatungstates, Silica-Included Decatungstates, and Silica-Supported Decatungstates

	σ (cm^{-1})							
sample	Si−O−Si	W=O	W−O−W					
$Q_4W_{10}O_{32}$	—[a]	994	959	891	800	662	582	435
$Na_4W_{10}O_{32}$	—[a]	995	960	893	799	661	585	433
Q**1**	1081	—[b]	957	881	810	655	575	463
Na**1**	1080	—[b]	949	881	791	669	578	465
Q**2**	1080	—[b]	961	894	801	661	581	445
Na**2**	1081	—[b]	962	892	800	660	583	441

[a] Not found. [b] Covered by Si−O−Si vibrations.

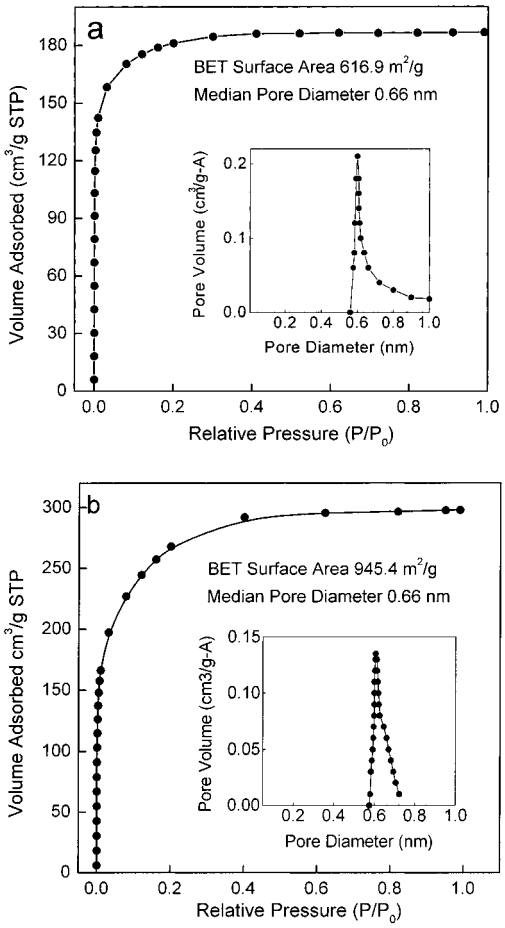

Figure 2. Nitrogen adsorption isotherms and pore size distribution curves for (a) $Na_4W_{10}O_{32}/SiO_2$ and (b) $Q_4W_{10}O_{32}/SiO_2$.

vibration bands are assigned to the chemical interactions between the $M_4W_{10}O_{32}$ molecule and the silica network as described above.

The surface textural properties of Na**1** and Q**1** were assessed by nitrogen adsorption measurements at 77 K, and the nitrogen adsorption isotherms and pore size distributions are presented in Figure 2. Three lines of evidence allow us to confirm microporous structures of Na**1** and Q**1**. First, most of the adsorption took place at the very low pressure, i.e., $P/P_0 \leq 0.1$. Second, very high BET specific surface areas were achieved for Na**1** (617 $m^2\ g^{-1}$) and Q**1** (945 $m^2\ g^{-1}$). High specific surface areas of Na**1** and Q**1** would result in high catalytic activity because the active sites (W−O−W bonds) were better spread on the surface and in the micropores of the silica matrix. Third, the median pore diameter is 0.66 nm for Na**1** and 0.65 nm for Q**1**. Formation of a microporous structure in Na**1** or Q**1** originates from the mesoporous

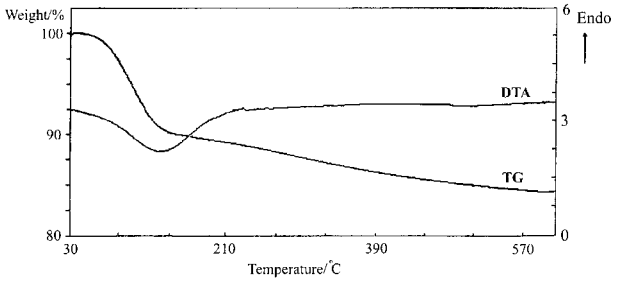

Figure 3. TG and DTA trace of $Na_4W_{10}O_{32}/SiO_2$.

structures of the silica particulate gel (median pore diameter is 3.8 nm).[22] During the course of hydrolysis of TEOS in the presence of decatungstate at pH 2.0 ± 0.2, $Na_4W_{10}O_{32}$ or $Q_4W_{10}O_{32}$ was entrapped by the silica network, leading to a decrease of the pore sizes and formation of a $Na_4W_{10}O_{32}/SiO_2$ or $Q_4W_{10}O_{32}/SiO_2$ composite with micropores. The silica network seemed to be narrow enough to prevent the removal of $Na_4W_{10}O_{32}$ or $Q_4W_{10}O_{32}$ molecules from it.

The thermal stability of Na**1** and Q**1** was examined by simultaneous TG/DTA experiments (Figure 3). The first weight loss (10% in Na**1** and 9.2% in Q**1**) from 30 to 135 °C was attributed to losing surface water and excessive 1-butanol. The boiling point of 1-BuOH is 117 °C, so it cannot be removed completely by water washing. The second weight loss (3.9% in Na**1** and 4.6% in Q**1**) from 330 to 550 °C was attributed to losing the constitutional water from $(\equiv Si-OH_2^+)(M_3W_{10}O_{32}^-)$, which would result in the decomposition of decatungstates.

Particle sizes of Na**1** and Q**1** were estimated by SEM images (Figure 4). From the imagines we can see that particles of Na**1** are well distributed. As for Q**1**, the distribution of particles is uneven. The particle size for both of them is ca. 20−40 nm.

Photochemical Behavior. The photocatalytic activity of Na**1**, Q**1**, Na**2**, and Q**2** was tested via degradation and mineralization of trace TCF (40 mg/L) in aqueous solution and at atmospheric pressure (Figure 5). Conversion of TCF into Cl^- ion was 7% after irradiating aqueous TCF for 5 h, suggesting that TCF did not undergo significant photolysis in the absence of the catalyst. Nor did we observe any significant reaction between TCF and $W_{10}O_{32}^{4-}$ in the dark (neither Cl^- nor $H_2PO_4^-$ ion being detected). However, a significant conversion was observed with irradiation of Na**1** suspension in the near-UV area, suggesting that mineralization of aqueous TCF resulted from photoexcitation of Na**1**.

The photocatalytic activity of $W_{10}O_{32}^{4-}$ originates from its unique structure. First, $W_{10}O_{32}^{4-}$ ions have similar electronic attributes to that of semiconductor TiO_2. Both of them have large band gaps, i.e., HOMO−LUMO gaps for microporous decatungstates are ca. 3.6−3.8 eV (estimated by UV/DRS), and the band gaps of TiO_2 are 3.2 eV. Second, $M_4W_{10}O_{32}$ and TiO_2 both have d_0 transition metal and oxygen atom. UV irradiation of $W_{10}O_{32}^{4-}$ resulted in the formation of O→W CT excited state $[W_{10}O_{32}^{4-}]^*$ with considerable oxidizing capacity (ca. 2.5−2.6 eV vs the NHE).[16] Thus, decatungstates that are otherwise thermally inactive to degrade TCF become a powerful oxidant under the photoreactivation by the near-UV light. By using semiconductor

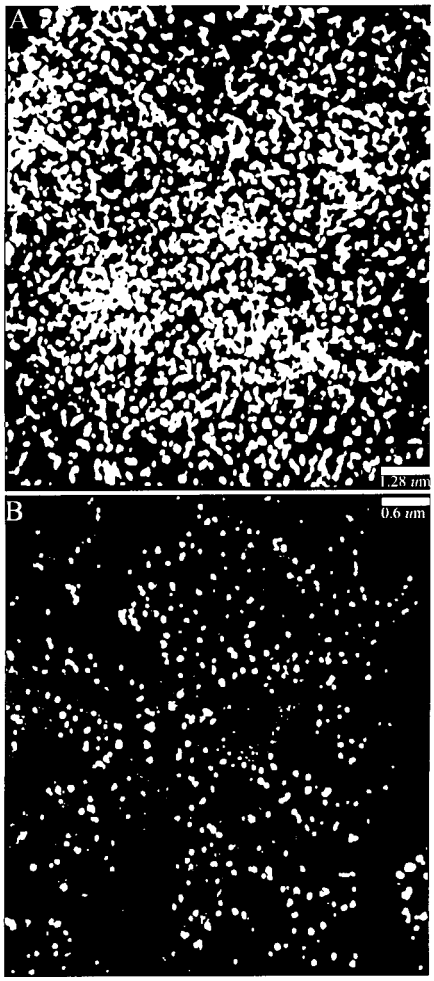

Figure 4. SEM images of (A) $Na_4W_{10}O_{32}/SiO_2$ and (B) $Q_4W_{10}O_{32}/SiO_2$.

notation, $[W_{10}O_{32}^{4-}]^*$ can be presented by

$$W_{10}O_{32}^{4-} + h\nu \rightarrow [W_{10}O_{32}^{4-}]^* \leftrightarrow W_{10}O_{32}^{4-}(e^- + h^+) \quad (3)$$

Thus, initiating the oxidation reaction by $W_{10}O_{32}^{4-}$ which is presented in

$$[W_{10}O_{32}^{4-}]^* + TCF \rightarrow W_{10}O_{32}^{5-} + TCF_{ox} \quad (4)$$

During this process, TCF was oxidized by $[W_{10}O_{32}^{4-}]^*$ to TCF_{ox}, while $W_{10}O_{32}^{4-}$ was reduced into the mixed-valence blue complex ($W^VW_9^{VI}O_{32}^{5-}$) by obtaining one electron from TCF. Formation of $W_{10}O_{32}^{5-}$ originated from the intervalence ($d_0 \rightarrow d_1$) charge transfer (IVCT), and it is referred to as a heteropoly blue (HPB). The HPB was confirmed by UV/DRS (Figure 1b), i.e., absorption at 774 nm (IVCT band) is the characteristic of $W_{10}O_{32}^{5-}$. The result also shows that only one-electron reduced form of $W_{10}O_{32}^{4-}$ was yielded for this reaction, because the IVCT band for the two-electron reduced form of $W_{10}O_{32}^{4-}$ is at 622 nm.[7]

Reoxidation of $W_{10}O_{32}^{5-}$ to its original oxidation state ($W_{10}O_{32}^{4-}$) was easy by electron acceptor such as dioxygen dissolved in the suspension. This process is presented by

$$2W_{10}O_{32}^{5-} + 2H^+ + {}^1/_2O_2 \rightarrow 2W_{10}O_{32}^{4-} + H_2O \quad (5)$$

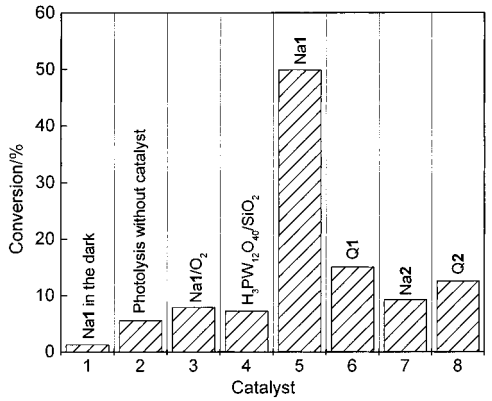

Figure 5. Mineralization of TCF into Cl^- ion under various conditions. $[TCF]_0 = 40$ mg/L; 0.2 g of the catalyst was used in each catalytic cycle; conversion (%) = $(1 - [Cl^-]_t/[Cl^-]) \times 100$, where $[Cl^-]_t$ represents the concentration of Cl^- ion at an elapsed time of reaction and $[Cl^-]$ represents the total concentration of Cl^- ion; and the irradiation time was 4 h. Data obtained are the average values of three runs.

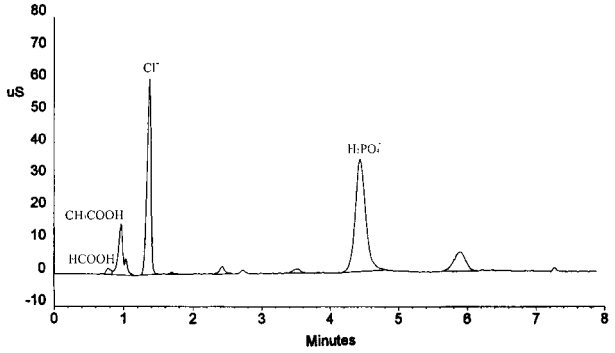

Figure 6. Ion chromatographic effluent curve for TCF photocatalytic degradation products. The suspension (TCF + Na**1**) was irradiated by high-pressure mercury lamp for 2 h.

Having undergone the above two steps (eq 4 and eq 5), a net photocatalytic cycle was completed. The reoxidized form ($W_{10}O_{32}^{4-}$) was then capable of engaging in another series of electron transfers that may continue until TCF was mineralized completely. The mechanism by which heterogeneous Na**1** photocatalytically oxidized aqueous TCF compounds is described in the next section.

Under the same conditions, the photocatalytic activity of the Q**1**, Na**2**, or Q**2** was lower than that of Na**1**. The reason is the leakage of $W_{10}O_{32}^{4-}$ from the catalyst support, silica matrix, during the photocatalytic process. After irradiation of the suspension for 2 h, the pH value of the suspension decreased from the original 6.8 to 3.5 because of the formation of organic acids, HCOOH and CH_3COOH, and HCl (Figure 6). Under this acidity, the dropped $W_{10}O_{32}^{4-}$ ion was decomposed into α-Keggin and β-Keggin $H_2W_{12}O_{40}^{6-}$ ions.[45] Decomposition of $W_{10}O_{32}^{4-}$ also can be evidenced by UV absorption spectrum. That is, after finishing the irradiation, the blue suspension was allowed to be centrifuged as soon as possible in the closed vessel, and then the clear solution was separated from the solid catalyst. In the case of the clear solution, absorption at 199, 266, and 774 nm was measured, indicating that the system contained mixed valence of W atoms. That is, W^V (774 nm, IVCT band of $W_{10}O_{32}^{5-}$ ion) and W^{VI} (199 and 266 nm, attributed to W═O and W−O−W CT band of Keggin ions) cluster ions exited simultaneously. At the

same time, the characteristic absorption of $W_{10}O_{32}^{4-}$ disappeared totally, because the dropped $W_{10}O_{32}^{4-}$ ion transferred into either $W_{10}O_{32}^{5-}$ or $H_2W_{12}O_{40}^{6-}$ ion during the course of photooxidation of TCF. Decomposition of $W_{10}O_{32}^{4-}$ ion resulted in the decrease of the photocatalytic activity of Q**1** significantly.[5] In the case of the Na**1**, the leakage was hardly observed because the chemical interaction between $Na_4W_{10}O_{32}$ molecule and the silica network was strong. In addition, $Na_4W_{10}O_{32}$ molecules were totally entrapped into the silica network during sol−gel process, and narrow silica network prevented the removal of $Na_4W_{10}O_{32}$ molecules from them. Therefore, Na**1** exhibited the highest activity for photodegradation of TCF. In the case of the Q**1**, electrostatic force interaction between large counterion, nBu_4N^+, and $W_{10}O_{32}^{4-}$ anion is strong, resulted in weakly chemical interaction between the ≡Si−OH group and the $Q_4W_{10}O_{32}$ molecule. Therefore, formation of ($\equiv Si-OH_2^+$)-($Q_3W_{10}O_{32}^-$) was difficult and the drop of $Q_4W_{10}O_{32}$ happened. In the case of the silica-supported decatungstates, Na**2** and Q**2**, the leakage of the decatungstates into the reaction system is inevitable, because only electrostatic interactions between the decatungstate molecule and the ≡Si−OH group existed in both of the composites. The photocatalytic activity of Na**1** was also compared with that of the $H_3PW_{12}O_{40}/SiO_2$. The lower photocatalytic activity of the $H_3PW_{12}O_{40}/SiO_2$ is due to its higher HOMO−LUMO gaps (4.5−4.9 eV, estimated by UV/DRS). Therefore, transition from the ground state to the excited state was more difficult, which resulted in lower photocatalytic efficiency.[5]

The above experiments were performed under atmospheric pressure. When the suspension was saturated with oxygen, mineralization of TCF into Cl^- ion over the Na**1** decreased greatly. This is explained as follows. In the presence of pure oxygen, reoxidation of $W_{10}O_{32}^{5-}$ to $W_{10}O_{32}^{4-}$ was so rapid that the photooxidation of TCF with Na**1** was retarded severely. Therefore, TCF was only photodegraded into organic acids but not mineralized into CO_2 and H_2O continuously. The result is similar to that of Maldotti's; i.e., in the presence of 760 Torr of O_2, silica-supported $H_3PW_{12}O_{40}$ or $(nBu_4N)_4W_{10}O_{32}$ can photooxidize cyclohexane to cyclohexanone and cyclohexanol without causing mineralization processes.[20] To obtain total mineralization of TCF over Na**1**, the dissolved oxygen from atmosphere is more suitable.

Mechanistic Considerations. It is generally accepted that in aqueous suspension, the primary photocatalytic pathway for TiO_2 is the oxidation of adsorbed water to form OH• radicals.[38,39] With respect to polyoxotungstates, the reason is unclear. Yamase, Papaconstantinou, and Hu have reported that photooxidation of organics with polyoxotungstates also performed via OH• radicals.[2,11,22] However, Hill and co-workers thought that soluble polyoxotungstates oxidize the substrates in organic solvents via a direct electron transfer.[4,6,7] In our current work, according to major intermediates detected by ES-MS and IC (Figure 6), the pathway of photooxidation of aqueous TCF over the heterogeneous photocatalytic material, Na**1**, may be inferred via OH• radicals. Equations 6−9 present the process of formation of OH• radicals during photooxidation of aqueous TCF over Na**1**. That is, light absorption induced the creation of

Scheme 1. Proposed Hydroxyl Radical-Mediated Photodegradation Mechanism of TCF over Na1

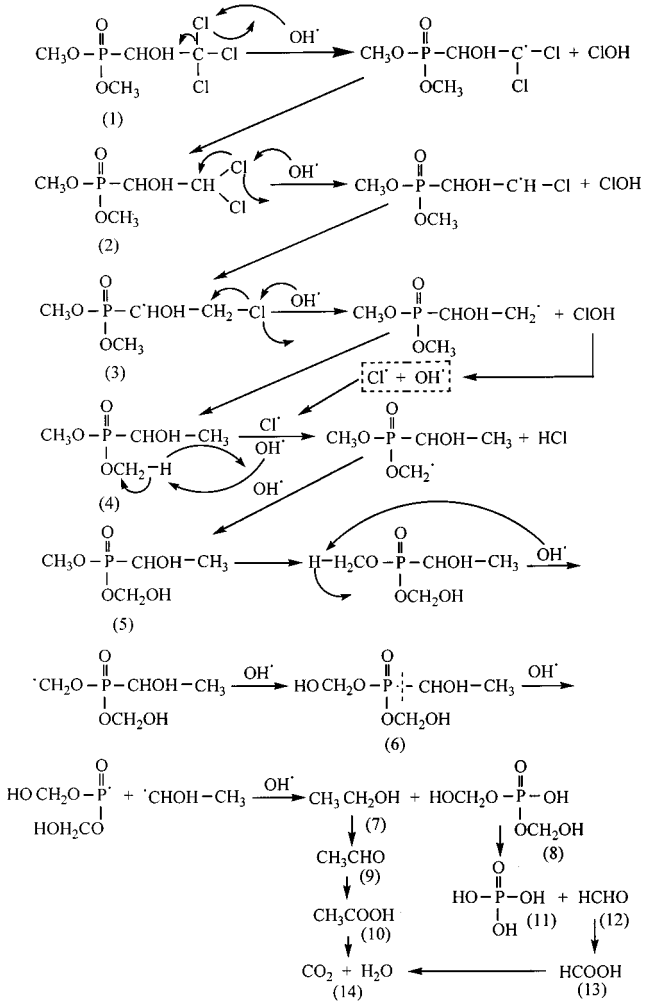

electron−hole pairs, and then the holes reacted with OH^- groups coming from water to generate OH• radicals.

$$W_{10}O_{32}^{4-}(e^- + h^+) + H_2O \leftrightarrow W_{10}O_{32}^{4-}(e^-) + OH^\bullet + H^+ \quad (6)$$

$$W_{10}O_{32}^{4-}(e^-) + O_2 \rightarrow [W_{10}O_{32}O_2]^{5-} \quad (7)$$

$$[W_{10}O_{32}O_2]^{5-} \rightarrow W_{10}O_{32}^{4-} + O_2^- \quad (8)$$

$$O_2^- + H^+ \rightarrow HO_2 \quad (9)$$

OH• radicals thus formed are very strong and unselective oxidants ($E_0(OH^\bullet/H_2O) = 2.58$ V vs NHE at pH 3)[46] and are responsible for total oxidation of TCF. In addition, O_2^-/HO_2 species thus formed might be important in the degradation and final mineralization of the intermediates. The proposed mechanism of photooxidation of TCF over microporous decatungststse, Na**1**, is shown in Scheme 1.

The first, successive cleavage of C−Cl bonds happened corresponding to Cl abstraction from TCF one by one, leading to ClOH. This step is supported by ES-MS. That is, the molecular ion peak or fragment peaks with m/z 257.1 (259.1), 220.7 (222.7), 188.4 (190.4), and 154.0 (156.0) were detected, where $m = (M + H)^+$ and M = molecular weight (abbreviated MW). Therefore, the MW

(46) Schwarz, H. A.; Dodson, D. W. *J. Phys. Chem.* **1989**, *93*, 409.

of the corresponding compounds were calculated. From MW we infer that compounds **1**−**4** in Scheme 1 existed in the suspension (irradiation time is 1 h). ClOH is unstable, and it can decompose into Cl• and OH• radicals rapidly. Second, H abstraction by Cl• radicals from compound **4** led to HCl and phosphonate radical cation. The latter may subsequently oxidized by OH• radicals to oxygenated products (**5** and **6** in Scheme 1). These products were oxidized continuously, corresponding to the cleavage of C−P bond and leading to ethanol (**7**) and compound **8**. At last, ethanol was continuously oxidized to aldehyde (**9**), acetic acid (**10**), and then the final products CO_2 and H_2O. At the same time, compound **8** was oxidized to phosphonic acid (**11**) and formaldehyde (**12**), respectively. Formaldehyde was continuously oxidized to formic acid (**13**) and then CO_2 and water (**14**). At pH ca. 3.5, $H_2PO_4^-$ anion was detected. The second step is supported by IC analysis.

Besides the above-mentioned, adsorption appears to play a key role in heterogeneous photocatalyst chemistry, and rapid diffusion of the reactants into the micropores of the catalyst may achieve high photoactivities, so that the mineralization may be performed by direct oxidation via $[W_{10}O_{32}^{4-}]^*$. Further research will confirm it.

The overall reaction is shown as follows

$$(CH_3O)_2P{=}O{-}CHOH{-}CCl_3 + {}^9/_2O_2 \xrightarrow[Na\mathbf{1}]{h\nu} 4CO_2 + 3Cl^- + H_2PO_4^- + 4H^+ + H_2O \quad (10)$$

Conclusion

Decatungstates are the most photochemically reactive polyoxometalates, and their photochemical behavior has been extensively studied in homogeneous systems. Here, we used a sol−gel technique to prepare a water-insoluble $Na_4W_{10}O_{32}/SiO_2$ composite with a microporous structure. The purpose is to obtain a kind of heterogeneous polyoxometalate photocatalyst for practical applications. Under near-UV irradiation, mineralization of aqueous TCF into CO_2, H_2O, and other inorganic ions such as Cl^-, $H_2PO_4^-$, and H^+ over the $Na_4W_{10}O_{32}/SiO_2$ composite was achieved under atmospheric pressure, whereas only degradation took place under saturated oxygen. The leakage of $Na_4W_{10}O_{32}$ from the support was hardly observed, and the system was handled at natural acidity (not at pH < 3) because $W_{10}O_{32}^{4-}$ was entrapped by the silica network, and the narrow silica network prevented them from being removed. Photooxidation of aqueous TCF over heterogeneous photocatalyst, $Na_4W_{10}O_{32}/SiO_2$ composite, may be due to OH• radical attack that was inferred from the product distributions.

Acknowledgment. The Natural Science Fund Council of China is acknowledged for financial support (Grant No. 20071007). The present work is also supported by the Foundation for University Key Teacher by the Ministry of Education of China.

CM010211I